Observations of Potential Gaia DR2 Red Dwarf Binary Stars in the Solar Neighborhood – II

Ivan Altunin[1], Rick Wasson[2], and Russell Genet[3]

1. University of California, Berkeley, ialtunin@berkeley.edu
2. Orange County Astronomers, Murrieta, California, ricksshobs@verizon.net
3. California Polytechnic State University, San Luis Obispo, rgenet@calpoly.edu

Abstract: Astrometric and photometric observations of double stars within 100 parsecs of the Earth, which included a late K or M dwarf component, were made in Sloan g' r' i' z' filters with the Orange County Astronomers 22-inch telescope in 2019 using quasi-speckle interferometry techniques where exposures up to 1 second long were processed with standard speckle bispectrum methods. This paper reports continuation of those observations in 2020 for 12 more binaries at the Fairborn Institute Robotic Observatory's remotely accessed 11-inch telescope. Longer quasi-speckle integrations—up to 5 seconds—were used with a telescope of half the aperture and 1/4 the photon-capturing area, reaching about the same faint magnitudes (G=14.8) without introducing too much atmospheric smearing. Gaia summary data are reviewed for the observed stars, bispectrum reconstructed images are presented, astrometric and photometric results are reported, and details of several systems are discussed.

Introduction

Although the Red Dwarf (RD) stars—spectral types late K and M on the Main Sequence—are the most common stars in the Milky Way, they are intrinsically faint and more difficult to observe than earlier types, so their population, even within the Solar Neighborhood, has not been fully explored (Cooper 2019). Recent advances in low cost, red-sensitive, high speed but low-read-noise, back-side illuminated CMOS cameras has enabled the study of brighter RD stars with small telescopes. Astrometric observation of binaries with one or both components being a RD can lead to orbital solutions and the determination of the mass ratio of the two stars, while photometry of the binary components can provide approximate temperatures and spectral types. Taken together, these observations can provide estimates of the mass of each star (Davidson et al. 2009). The RECONS survey has completed the census of all stars within 10 parsecs of the Sun, and the campaign to discover all the stars within 25 parsecs is continuing (Winters et al. 2019).

A campaign to observe the brightest nearby binary systems containing a RD was initiated with the Orange County Astronomers 22-inch telescope in 2019 (Wasson et al. 2020, hereinafter RDSN-I). The observations presented here continue that program, using the same target list, filters, and data reduction methods, but a telescope with half the aperture, the 11-inch telescope at the Fairborn Institute Robotic Observatory (FIRO).

Targets included systems containing one or two RD components already in the Washington Double Star (WDS) catalog, as well as systems not in the WDS but in the Gaia Double Star (GDS) data base derived from Gaia Data Release 2 (DR2). Most of these systems have few previous observations—often by large-scale surveys such as SDSS and 2MASS, which have limited resolution (because of over-exposure in very deep images) to obtain separation and position angles between the components or multi-band photometry of the individual components. The current observations offer confirmation of the previous astrometric observations, the possibility of detecting orbital motion, and new Δ magnitudes in the Sloan bands.

The Gaia astrometric/photometric satellite has provided observations for a comprehensive stellar catalog, Gaia DR2, which was made public in 2018. A sub-catalog, GDS1, has been developed (Rowe 2018) that contains 6.8 million Gaia double stars suitable for observation with smaller telescopes with separations less than 10". The accompanying GDS1 Tool was used to locate potential binary stars in the Solar neighborhood

Observations of Potential Gaia DR2 Red Dwarf
Binary Stars in the Solar Neighborhood – II

that had accurate parallaxes, proper motions, and color indices, and might contain a RD star.

Using GDS1, all stars with parallax greater than 10 milli-arcsec (100 parsecs) as well as those in the southern sky (to avoid high airmass) were discarded, still leaving several thousand double star candidates. Potential binaries, as opposed to chance optical doubles, were identified as pairs having very nearly the same Gaia parallax and similar proper motion.

The Gaia H-R diagram, published as part of DR2, shows that the division between K and M dwarfs occurs at Gaia color index (Bp-Rp) = 2.3. Therefore, systems that possibly contain a RD (late K through M) were identified by (Bp-Rp) > 2. Luminosity class was assumed to be normal main sequence dwarf (V) because none of these systems contained a component brighter than 10th magnitude. Thirty-five of the brightest candidates were observed in RDSN-I; about half of these were not found in the Washington Double Star Catalog (WDS) and may be considered "new" Gaia double stars. An additional dozen candidates were observed in RDSN-II (this paper) with, again, half not being in the WDS, although all but one of these were found in the newly revised Washington Double Star Supplement (WDSS), which was not surprising since many of the WDSS entries consist of just Gaia observations of both components.

Quasi-speckle interferometry employs a single reference star for deconvolution, and bispectrum analysis of double star observations for recovery of phase information distorted by the atmosphere. Quasi-speckle interferometry appears to provide better results than either simple stacking or lucky imaging. This somewhat surprising result may be due to: (1) the retention of some moderate-scale information in these somewhat longer-exposure images which can be correlated by speckle processing better than by stacking or lucky imaging; (2) single-star deconvolution which can, to some extent, cancel optical aberrations and systematic atmospheric phenomena such as dispersion, and (3) processing of the observations in the Fourier frequency domain which allows suppression of noise at spatial frequencies that cannot be real, e.g., smaller than the Airy disk or larger than the frame size.

Objective

The primary objective of this project was to continue the astrometric and photometric observations in multiple Sloan filters begun in RDSN-I on the OCA 22-inch telescope. The OCA telescope became temporarily inoperative due to equipment difficulties.

The second objective was to determine whether the quasi-speckle interferometry technique could be extended to observations with a telescope of half the aperture (11 inches) and $1/4^{th}$ the photon-capturing area. Hopefully, the same faint magnitudes could be reached, albeit with longer integration times and without introducing too much atmospheric smearing.

The third objective was to further refine remote real-time speckle interferometry observational techniques. These observations were initiated by Marchetti et al. (2020) on the 11-inch telescope at the Fairborn Institute Robotic Observatory (FIRO).

Image Processing Technique

In the previous RDSN-I observations with the OCA 22-inch telescope, it was originally hoped that speckle interferometry could be employed for diffraction-limited observations ($\rho > 0.35$" in the i' band) which might reveal additional RD stars unresolved by Gaia. However, because of the short exposures required to "freeze" the seeing and preserve the diffraction-limited speckle information in each frame, very few of the RD binaries were bright enough to be observable with such short exposures. Thus, most candidates required longer exposures, up to 1 second. These long exposures were blurred by atmospheric motion, and thus were seeing-limited rather than diffraction-limited.

Nevertheless, speckle processing techniques were still found to be useful – capable of resolving stars more clearly with separations at or somewhat below the seeing limit. Apparently, there is still information about the large-scale structure (and perhaps some small-scale structure as well) in these long-exposure images, which can be correlated by speckle processing better than the usual methods of stacking or lucky imaging. The observation of a single star used for mathematical deconvolution in speckle processing—standard practice in speckle interferometry—can, to some extent, cancel optical aberrations and systematic atmospheric phenomena such as dispersion. Finally, using all the frames probably increases signal/noise if most of them contain some valid image information. Further exploration of the quasi-speckle interferometry technique is planned.

Instrumentation and Procedures

The Fairborn Institute Robotic Observatory (FIRO) is equipped with the 11-inch telescope shown in Figure 1. The optics are Celestron C-11 Schmidt Cassegrain with an f/10 focal ratio and an effective focal length of 2800 mm. The custom equatorial "L" mount was designed and built in conjunction with California Polytechnic State University students and staff. A Sidereal Technology Servo Controller II controls the telescope.

Observations of Potential Gaia DR2 Red Dwarf
Binary Stars in the Solar Neighborhood – II

Figure 1: The "L" of the L mount is on the left sitting on top of an equatorial wedge, while the Celestron C-11 optics is on the right.

The instrument payload, shown in Figure 2, consists of a focuser, filter wheel, and camera. The Clement "scissors" focuser is controlled by a gearhead servomotor and a second Sidereal Technology Servo Controller II. The five-position ZWO motorized filter wheel contains a clear "filter," and four Sloan filters: g', r', i', and z'. The CMOS camera is a thermoelectrically-cooled (40-50°C below ambient) ZWO ASI 1600 MM, selected for its low read noise (only 1.2e), small pixel size (3.8 microns), and relatively large format (16 megapixels, 4636x3520).

Figure 2: The instrument cluster includes a Clement focuser, a ZWO filter wheel, and CMOS camera.

Although the pixel scale of approximately 0.28"/pixel is somewhat under-sampled, the full-frame field-of-view of 21.5x16.3 arcminutes allows plate solutions for precise positioning and astrometric calibration to be made without the need for a second, wider-field camera. This one-camera-does-it-all compromise results in

the double star separation limit for the system being ~ 1.0" instead of the diffraction limit of ~ 0.6".

The Windows 10 computer, located in a cabinet just below the telescope, is a Dell OptiPlex 7070 with an Intel Core i7-9700 (8 cores operating at 4.7 GHz), 16GB DDR4 memory, an internal 256GB solid state drive, and two external (USB 3.2) 256GB solid state drives. Remote access to the system is via a static Internet IP address.

Speckle interferometry observations are made remotely in real time using a Sidereal Technology software program, SiTech ZWOCam, that controls the camera, filter wheel, focuser, and telescope. The program's ability to capture short exposures at high speed is critical for speckle interferometry. PlateSolve 3 allowed targets to be precisely centered within a selectable, small region of interest. An automatic focusing subroutine provides sharp images. Finally, a scripting feature allows a sequence of observations with different filters and integration times to be repeated any desired number of times.

Remote Observation Methods

A typical observing sequence began with manually opening the observatory and powering the equipment. The remotely located observers were connected to FIRO's computer over the Internet via AnyDesk. SiTech ZWOCam was launched, and the camera, filter wheel, and focuser activated.

The telescope was then unparked and tracking was initiated. Since the telescope is parked within the allowed observing window, an automatic focus routine and plate solution readies the telescope for observations before slewing to the first target. After the target coordinates were entered, the telescope moved to the target and, after another plate solution and a short move within the same full field, the target was always near the center of a small region of interest (RoI), typically 256x256 pixels (about 70"x70").

An imaging sequence was set up that included the exposure times, camera gain, and number of exposures for each filter in the sequence (typically a few hundred to a thousand). This filter sequence was set to repeat the desired number of times (typically five) to provide error statistics and improved precision. A path for storing images on an external drive was defined, and the observations were initiated. During the observations, small corrections in RA were sometimes required to keep the target near the center of the region of interest. After the sequence was completed for the double star, the coordinates of the reference star were entered, and the entire process was repeated, although only one sequence in each filter was required for deconvolution.

Observations of Potential Gaia DR2 Red Dwarf
Binary Stars in the Solar Neighborhood – II

Astrometric Calibration

Pixel scale and camera orientation calibration were accomplished with the Plate Solving feature of the SciTech ZWOCam program. As noted above, a full frame image of the target field, roughly 21'x16', was routinely taken to locate the center of the field after a slew. The solution relied on the UCAC4 Catalog stars to magnitude ~15. Typically, in 5-second exposures, 50 to several hundred stars were available for solution, yielding high accuracy.

The instrumentation was not touched during the several weeks of observation, so the calibration was very repeatable. The calibration was checked each night, and a total of ten Plate Solve frames were saved and processed again to provide overall statistics. The average pixel scale was 0.2779"/pixel ± 0.0004. The average camera orientation on the sky, which had been carefully aligned prior to the observations, was 0.092 degree ± 0.039. Because the camera angle correction was so small (<0.1 degree) compared with the uncertainty of PA measurements, it was ignored in the results shown in Table 2.

Data Reduction

This research made use of Speckle Toolbox 1.14 (Rowe 2020) using the bispectrum analysis (BSA) method so that the target components could be resolved as individual stars, enabling our measurements without the 180o ambiguity of autocorrelation. The first step in the data reduction was to take all the images of each star in each filter and process them into a single FITS Cube. Bispectrum analysis was initiated by taking the Fourier transform and calculating the triple correlation coefficients for all images in each FITS cube. These coefficients were then averaged, and the average power spectrum was also calculated. The bispectrum phase was then reconstructed by iteration to form the image. Photon bias was removed, and the image sharpened with adjustment of the Gaussian lowpass and high-pass filters. Finally, the astrometry and photometry measurements were obtained as shown in Figure 3.

Doubles Observed

The Gaia DR2 characteristics of the doubles studied are summarized in Table 1. These pairs were chosen from the same target list developed for RDSN-I. The far-right column gives the WDS identification for those stars previously identified. "WDSS-n" indicates that the star is in the WDS Supplemental (WDSS) Catalog, and "n" is the number of previous observations given there. Most of the WDSS stars were first identified as double by the Gaia satellite in DR2. Stars that have r > 3" may have been imaged, but not identified, by earlier surveys,

thus providing potential additional astrometric and photometric measures. WDSS-1 indicates that only the single Gaia observation had been reported before the new measures in this paper.
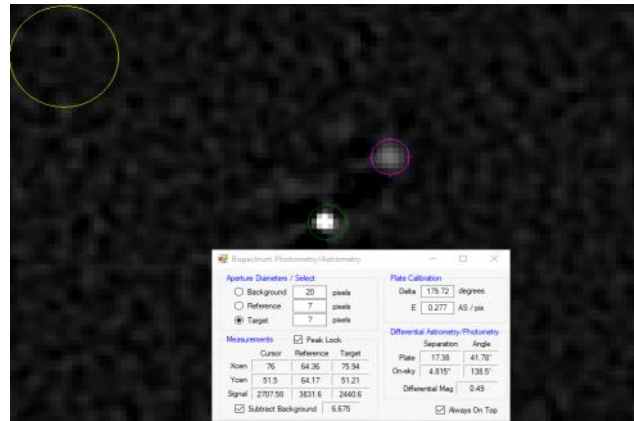

Figure 3: The final step in the bispectrum analysis reduction is astrometric and photometric measurement of the system. The green circle is the astrometric/photometric aperture for the Primary star ("Reference"), which is always centered in the image. The purple aperture is for the secondary star ("Target"), and yellow for the Background. The average Background pixel ADU level is subtracted from the ADU signal of each pixel within the star apertures; the two apertures must be the same size for proper photometric measurement of Δ magnitude.

Observations

Observations made of the target stars in Table 1 are shown in Table 2. Only a single observation, consisting of several hundred to a thousand frames, were made in each filter. Because most of these systems were faint (RD component 11 < G < 15), the quality of the observations varied widely, generally based on brightness of the secondary star at each wavelength, and on the seeing. Therefore, a Quality Code was included in Table 3, offered as an aid to interpreting these observations:

1. Good quality, comparable with moderate resolution speckle.

2. Lower quality, faint, or seeing-smeared images.

3. Marginal quality, because of low S/N of very faint or smeared images.

4. Poor quality, secondary star barely detectable above the noise.

5. Faint component not detected.

It was assumed that the measurements in separations and position angle did not change systematically in different wavelengths. Thus, the measurements in each filter were treated as "repeat" observations, allowing us to find the mean and standard deviation between them. This assumption has not been explored or proven and warrants further investigation.

Observations of Potential Gaia DR2 Red Dwarf
Binary Stars in the Solar Neighborhood – II

Coords (2000) UCAC4	ρ θ	G_A G_B	$(B_p-R_p)_A$ $(B_p-R_p)_B$	S_A S_B	$PMRA_A$ $PMRA_B$	PMD_A PMD_B	$π_A$ $π_B$	T_A T_B	WDS Disc	Period
170648.9+321159	3.279	10.779	1.822	K	53.2	-74.7	31.93	4153	WDSS-2	1206
612-054165	27.3	12.624	2.310	K/M	46.0	-82.8	31.93	3471		
173307.3+091437	4.689	9.199	1.401	K	31.0	-21.2	31.32	4522	WDSS-2	1905
497-071347	72.3	13.022	2.751	M	26.2	3.3	31.41	3757		
182740.7+501613	4.917	10.111	1.574	K	194.97	84.35	24.75	4231	18277+5016	2926
702-060220	236.7	12.14	2.568	M	200.44	86.87	24.3	3394	LEP 158	
183513.4+241839	2.468	11.644	2.415	M	-109.21	-273.73	39.70	3987	18352+2419	No Estmt
572-068539	4.6	12.419	2.608	M	-121.31	-277.05	39.63	3670	KPP3331	
184930.9+414635	4.179	9.624	1.195	G	-5.69	-21.11	20.37	4933	WDSS-1	2762
659-067595	89.5	12.303	2.352	K/M	-6.34	-24.81	20.57	3600		
185453.7+105842	3.808	8.793	1.750	K	29.56	132.01	53.77	4106	18550+1058	648
505-095824	44.9	11.437	2.586	M	29.48	84.21	53.88	3931	VYS8	
191659.0+022216	4.388	12.041	1.534	K	56.3	-23.8	10.24	4364	WDSS-3	No Estmt
462-091772	311.6	14.637	2.400	M	57.8	-24.4	10.36	3729		
192558.0+355453	6.038	9.083	1.164	G	-90.7	-161.0	25.03	4894	19260+3555	3461
630-070424	106.3	11.597	2.079	K/M	-100.0	-156.9	25.04	4046	BU 1286 AC	
195255.2+431624	5.091	10.081	1.203	G	121.7	106.5	16.30	4828	19529+4316	5266
667-080219	257.1	13.216	2.047	K/M	122.0	102.1	16.28	4185	KPP3349	
202201.6+214720	5.444	11.273	2.275	K/M	2.48	-131.67	37.17	3744	WDSS-3	2421
559-117009	67.46	**14.841**	**3.716**	**Late M**	4.67	-133.83	37.15	3590		
203335.4+385341	2.654	12.214	2.430	M	110.11	73.50	26.98	3398	20336+3854	1174
645-095063	79.39	12.375	2.458	M	103.95	56.08	27.16	3376	KPP4205	
204528.2+370546	4.892	12.228	1.945	K	60.30	6.66	11.56	4030	None	8660
636-098623	318.26	12.748	1.935	K	65.74	8.30	12.09	3933		

Table 1: Gaia DR2 characteristics of the candidate binaries observed. Left column: Primary RA and Dec coordinates for 2000.0 (hhmmss.s+ddmmss format)[above] and UCAC4 Catalog ID of Primary [below]. Column 2: Gaia DR2 separation (r) in arc-sec [above] and Gaia position angle (θ) in degrees [below]. The remaining seven columns give Gaia data for the Primary (A) [above] and Secondary (B) [below]: G magnitude, (Bp-Rp) Color Index, approximate Spectral Type based on the Gaia H-R diagram, Proper Motion in RA (mas/year), Proper Motion in Declination (mas/year), Parallax (mas), effective surface Temperature (K), WDS and Discovery designations if the pair is already recognized as a double star in the WDS Catalog (WDSS-n indicates an entry in the WDS Supplementary Catalog, where n is the total number of observations), and the estimated Period in years. Late M Dwarfs are noted in bold.

Observations of Potential Gaia DR2 Red Dwarf
Binary Stars in the Solar Neighborhood – II

Differential Photometry from Bispectrum
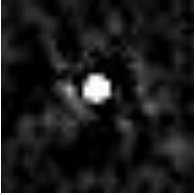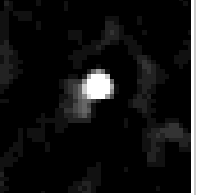
Analysis

For cool red stars, observations at longer wavelengths are useful not only because they produce most of their radiation in near-IR, but also because the atmospheric seeing is better, causing less distortion during exposures. The RDSN-I observations were made using Sloan filters (Astrodon Gen_2 interference filters), and the FIRO speckle instrumentation includes the same Sloan filter set from Astrodon. For the stars observed in this paper, the best combination of RD target/detector sensitivity/seeing was generally in the i' band.

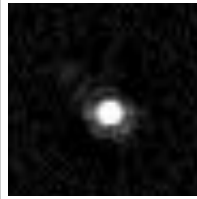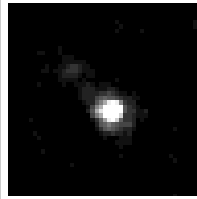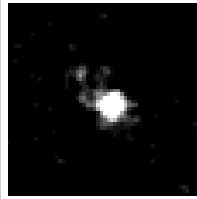Bispectrum analysis recovers the approximately correct flux and Δ magnitude in each filter. Bispectrum photometry is like the method typically used in CCD aperture photometry. The net flux "signal" for each star in the reconstructed image is the sum of ADU counts from all pixels inside a circular aperture centered on the centroid of the star, with the background level for the same aperture area subtracted. However, the background is measured in a separate "blank" area of the image, not in an annulus surrounding the star because of the likelihood that the companion star, the Airy rings, or other diffraction artifacts may fall in or near the annulus. The Δ magnitude (secondary-primary) is calculated automatically by STB from the ratio of net counts of each star.
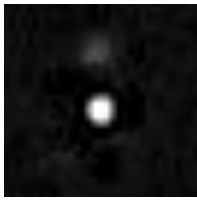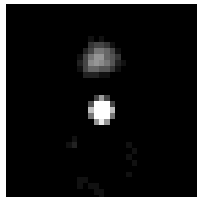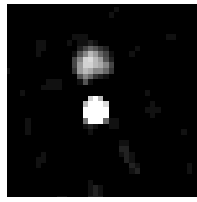
During reduction, the same photometry aperture was used for both stars, to capture the same proportion of light for each star; use of different apertures would contain different percentages of total light, causing an error in Δ magnitude. A large aperture that included all
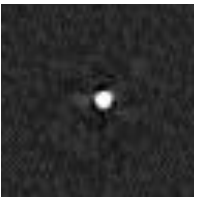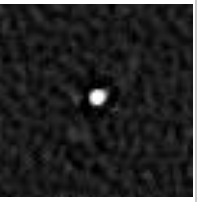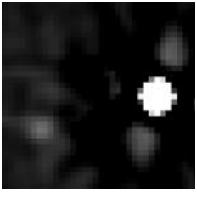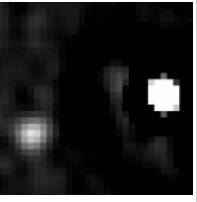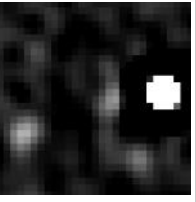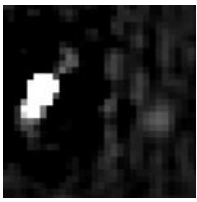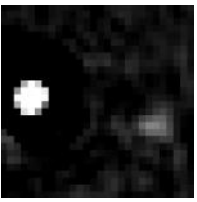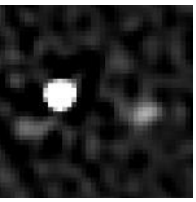
Date	Coord (2000)	Filter	θ	r	Δ Mag	Q
2020.589	173307.3+091437	Clear	70.82	4.487	4.61	4
	UCAC4 497-071347	r'	69.15	4.839	4.45	4
		i'	70.83	4.558	3.33	2
		z'	69.49	4.723	2.87	1
	Average		70.07	4.652		
	Std Dev		0.88	0.159		
	Filter	Clear	r'	i'	z'	
	Images					

Date	Coord (2000)	Filter	θ	r	Δ Mag	Q
2020.611	182740.7+501613	Clear	No Observations			
	UCAC4 702-060220	r'	238.56	4.910	3.50	4
	WDS: 18277+5016	i'	235.50	5.054	2.79	2
	Discov: LEP 158	z'	239.53	5.196	2.49	3
	Average		237.86	5.053		
	Std Dev		2.10	0.143		
	Filter	Clear	r'	i'	z'	
	Images					
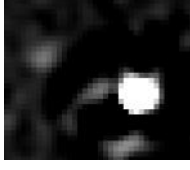
Observations of Potential Gaia DR2 Red Dwarf
Binary Stars in the Solar Neighborhood – II

Date	Coord (2000)	Filter	θ	r	Δ Mag	Q
2020.591	183513.4+241839	Clear	4.24	2.530	1.48	2
	UCAC4 572-068539	r'	5.19	2.465	1.45	2
	WDS: 18352+2419	i'	3.87	2.479	0.97	1
	Discov: KPP 3331	z'	6.24	2.401	1.30	1
	Average		4.89	2.469		
	Std Dev		1.06	0.053		
	Filter	Clear	r'	i'	z'	
	Images					

Date	Coord (2000)	Filter	θ	r	Δ Mag	Q
2020.600	184930.9+414635	Clear	No Observations			
	UCAC4 659-067595	r'	89.85	4.180	3.03	2
		i'	89.94	4.217	2.19	1
		z'	89.76	4.203	1.77	1
	Average		89.85	4.200		
	Std Dev		0.09	0.019		
	Filter	Clear	r'	i'	z'	
	Images					

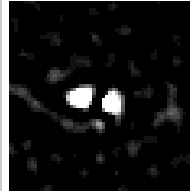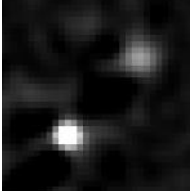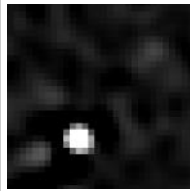| Date	Coord (2000)	Filter	θ	r	Δ Mag	Q
2020.600	185453.7+105842	Clear	No Observations			
	UCAC4 505-095824	r'	48.10	3.620	3.50	1
	WDS: 18550+1058	i'	47.26	3.735	2.76	1
	Discov: VYS8	z'	48.19	3.453	2.15	3
	Average		47.85	3.603		
	Std Dev		0.51	0.142		
	Filter	Clear	r'	i'	z'	
	Images					

Observations of Potential Gaia DR2 Red Dwarf
Binary Stars in the Solar Neighborhood – II

Date	Coord (2000)	Filter	θ	r	Δ Mag	Q
2020.611	191659.0+022216	Clear	No Observations			
	UCAC4: 462-091772	r'	311.61	4.198	3.47	2
		i'	312.18	4.667	3.39	2
		z'	Secondary Not Detected			5
	Average		311.90	4.433		
	Std Dev		0.40	0.332		
		Clear	r'	i'	z'	

Date	Coord (2000)	Filter	θ	r	Δ Mag	Q
2020.630	192558.0+355453	Clear	No Observations			
	UCAC4: 630-070424	r'	106.52	5.961	3.48	2
	WDS: 19260+3555	i'	106.15	5.972	2.66	1
	Discov:BU1286AC	z'	106.32	5.914	2.43	1
	Average		106.33	5.949		
	Std Dev		0.19	0.031		
		Clear	r'	i'	z'	

Date	Coord (2000)	Filter	θ	r	Δ Mag	Q
2020.622	195255.2+431624	Clear	No Observations			
	UCAC4: 667-080219	r'	255.92	5.109	3.58	2
	WDS: 19529+4316	i'	257.57	5.108	3.00	1
	Discov: KPP3349	z'	257.82	5.081	2.61	1
	Average		257.10	5.099		
	Std Dev		1.03	0.016		
		Clear	r'	i'	z'	

Observations of Potential Gaia DR2 Red Dwarf
Binary Stars in the Solar Neighborhood – II

Date	Coord (2000)	Filter	θ	r	Δ Mag	Q
2020.622	202201.6+214720	Clear	No Observations			
	UCAC4: 559-117009	r'	67.94	5.436	3.99	2
		i'	67.41	5.490	3.43	2
		z'	67.37	5.440	3.15	2
	Average		67.57	5.455		
	Std Dev		0.32	0.030		
		Clear	r'	i'	z'	

Date	Coord (2000)	Filter	θ	r	Δ Mag	Q
2020.611	203335.4+385341	Clear	No Observations			
	UCAC4: 645-095063	r'	80.65	2.650	0.69	1
	WDS: 20336+3854	i'	79.59	2.643	0.34	1
	Discov: KPP 4205	z'	79.99	2.628	0.24	1
	Average		80.08	2.640		
	Std Dev		0.54	0.011		
		Clear	r'	i'	z'	

Date	Coord (2000)	Filter	θ	r	Δ Mag	Q
2020.622	204528.2+370546	Clear	No Observations			
	UCAC4: 636-098623	r'	318.7	4.813	0.84	1
		i'	317.97	4.831	0.71	1
		z'	319.15	4.935	1.4	3
	Average		318.61	4.860		
	Std Dev		0.60	0.066		
		Clear	r'	i'	z'	

**Observations of Potential Gaia DR2 Red Dwarf
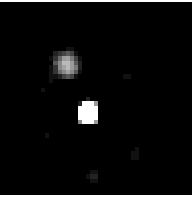Binary Stars in the Solar Neighborhood – II**
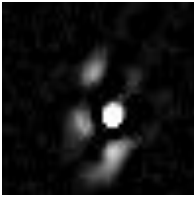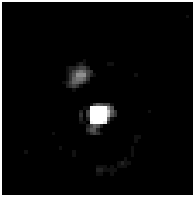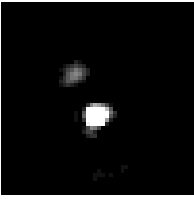
Date	Coord (2000)	Filter	θ	ρ	Δ Mag	Q
2020.591	170648.9+321159	Clear	26.15	3.222	2.09	3
	UCAC4 612-054165	r'	25.23	3.326	2.59	1
		i'	28.54	3.301	2.13	1
		z'	26.45	3.225	1.92	1
	Average		26.59	3.269		
	Std Dev		1.40	0.053		
	Filter	Clear	r'	i'	z'	
	Images					

Table 2: Observed characteristics of the stars using the BiSpectrum Analysis (BSA) method. The first column is the Besselian obser-vation date. Column 2 includes RA and Dec Coordinates (2000.0) in hhmmss.s+ddmmss format [above], and UCAC4 Catalog num-ber of the primary star [below]; WDS and discovery designations are also given for previously known doubles. The remaining col-umns are Filter, observed Position Angle (q) in degrees, observed Separation (r) in arc-sec, BSA Δ magnitude (secondary-primary), and Observation Quality Code (defined above). The Average and Standard Deviation results include all reported data, weighted equally regardless of quality. Reconstructed BSA images are shown in the last row for each system, oriented North up, East left.

the starlight was not used, because it could have included more background noise than real starlight at the outer edges. Typically, slightly larger aperture di-ameters were needed for the i' or z' filters because the size of the Airy disk grows in proportion to wavelength. This can also restrict astrometry and photometry of close pairs which approach the system's resolution. Ap-ertures must not overlap because the same light in the overlapping area would contribute to each star, biasing both the astrometry and photometry results.

Observations using the ZWO CMOS camera and Astrodon Sloan Gen_2 filter set should yield Δ magni-tudes roughly comparable with the Sloan Digital Sky Survey (SDSS) catalog. These filters match the pass-bands of the SDSS catalog reasonably well, and the CMOS silicon back-side-illuminated (BSI) sensor has similar sensitivity to the BSI CCD array used in SDSS, although spectral quantum efficiency (QE) response details are somewhat different. Instrumental photome-try was not transformed to the Sloan or any other stand-ard photometric system here, but these observations should supplement the Gaia G, Bp and Rp data.

For the red secondary stars observed here, the g'_2 filter generally gave low S/N and uncertain results in RDSN-I; the g' band was initially tried again in this study but was soon abandoned. However, the r'_2, i'_2, and z'_2 filters usually gave satisfactory results for the long exposures—up to 3 seconds in r' and i', and 5 sec-onds in z'—that were required for the faintest secondar-

ies (G~14.8).

The ZWO ASI 1600MM camera used here has a low-noise CMOS detector like the ZWO ASI 290MM used in RDSN-I, but the 1600 has a larger format, cooled sensor, and a different QE spectral response. Combining the filter transmission with the detector QE to estimate center wavelength (WL) and effective sensi-tivity for each filter are shown in Table 3.

The secondary stars observed were all quite red (Bp -Rp > 2.0 in Table 1); therefore, they should all be brighter at longer wavelengths. However, the z'_2 filter generally gave poorer images than in RDSN-I. This was probably caused by one or both of the following condi-tions: (1) the lower effective QE of the ZWO ASI 1600MM camera in the z' filter (Table 3) sometimes resulting in inadequate exposure, or (2) the wide sepa-ration of some pairs might have been outside the isopla-natic patch where the atmosphere could cause non-correlated movement of the two stars' seeing disks, which would diffuse and weaken the secondary star image when registered on the primary star. The effec-tive sensitivity of the 1600 CMOS camera which, like most CCD cameras is optimized for visible wave-lengths, is only about 10% at the center WL of the z' filter, whereas the 290 camera, which is optimized for near-IR sensitivity, has an effective sensitivity of about 32% in the z' filter, better suited for these faint RD stars.

**Observations of Potential Gaia DR2 Red Dwarf
Binary Stars in the Solar Neighborhood – II**

Filter	Center WL (nm)	FWHM (nm)	Max Transmission (%)	Effective QE (%)
Clear	~605	~360	95	48
g'	485	130	98	54
r'	624	130	98	49
i'	758	165	99	28
z'	880	232	99	10

Table 3: Results of Convolution of the ZWO ASI 1600MM camera quantum efficiency (QE) with transmission of the Clear and Astrodon Sloan Gen_2 filters. Columns are: filter, effective center wavelength, full-width-half-max transmission, maximum transmission, and effective QE at the center wavelength. QE characteristics of the ZWO ASI 1600MM camera were estimated from the Relative QE given in the Sony manufacturer literature, with Peak QE assumed to be 60%. QE was extrapolated beyond the 800nm limit given, to QE = 0 at 1050 nm.

Speckle differential photometry uncertainties of ~0.1 magnitude, primarily driven by Poisson statistics, have been reported for large telescopes (Horch et al. 2004), while uncertainties < 0.2 magnitude were found for small telescopes (Davidson et al. 2009). A Δ magnitude goal of ± 0.1 magnitude corresponds approximately to ±10% uncertainty. If both stars contribute equally to the uncertainty, then the flux of each star must be within ± 5% of the correct value. That is, the flux (or number of electrons counted) for each star must be within $1/20^{th}$ of the correct signal. If the error is driven primarily by photon statistics, then the net flux count for each star must be at least 400 electrons for uncertainty $< 1 \sqrt{400} < 1/20$. A high camera gain was generally used, giving ~0.2e-/ADU. Therefore, to achieve a signal of 400 electrons, the net ADU count within the photometry aperture must be greater than ADU ~ 400/0.2 ~ 2000. This net ADU count signal level was achieved for most of the primary stars, and some of the brighter secondaries in the i' and z' filters, but not for all secondary stars in the r' filter. Generally, of course, the fainter component will contribute the larger error for Δ magnitude.

Discussion

As listed in Table 1, six systems had previous entries in the WDS Catalog, and five of the remaining six were found in the WDSS. These are new Gaia discoveries, but were previously "data-mined" and were found in the WDS Supplement Catalog, recently placed on the WDS (and Georgia State University mirror) website. One system, **204528.2+370546**, discussed below, was found in neither catalog, so it is a new Gaia discovery first reported here.

Some of these systems have a separation greater than 3", where both stars may not be in the same isoplanatic patch. Depending on seeing, the two stars of a wide pair may be affected somewhat differently by different seeing cells. In principle, speckle processing adds the pixel brightness of the fainter star relative to the position of the brighter star; therefore in successive frames, the secondary star may appear in a slightly different position relative to the primary if moved differently by the atmosphere. This effect may produce a blurred or blotchy fainter representation of the secondary star. It may average out by taking many frames, but we generally acquired fewer frames (only a few hundred) as exposure times grew longer (greater than 1 second). Thus, even if averaged, differential atmospheric motion would spread the light of the secondary over a wider area, making it appear fainter. Although these adverse effects do not seem to have been too severe for the stars observed here, it could become a problem under other conditions.

Two of the systems previously observed in RDSN-I were observed again here, approximately one year later: **170648.9+321159** and **191659.0+022216**. Neither of these systems show movements beyond their standard deviation (σ) uncertainties, relative to Gaia or the 2019 RDSN-I measures. In Figure 4 two other systems do show movement greater than their 1σ uncertainties for θ, although not a strong statistical likelihood. These two systems are both close to us, making their movements easier to detect. Several other systems in Figure 5 have small θ or ρ uncertainties in the current measures. However, they have movements so small that no conclusion can be made about possible orbital motions until confirmed by further observations.

173307.3+091437 is apparently a new Gaia double star which has significant movement -2.2 ±0.9 deg in θ, seen at bottom of Figure 4. The separation uncertainty is much larger than the change since Gaia. This pair may have a large enough separation (~3.3"), to have been resolved in earlier large survey archives, yielding additional measures. The large Gaia parallax is 31.93

Observations of Potential Gaia DR2 Red Dwarf
Binary Stars in the Solar Neighborhood – II

only about 100 light years distant. The respective components are roughly K3V and M2V, based on the Gaia H-R diagram and (Bp-Rp) colors (1.401/2.751) in Table 1.
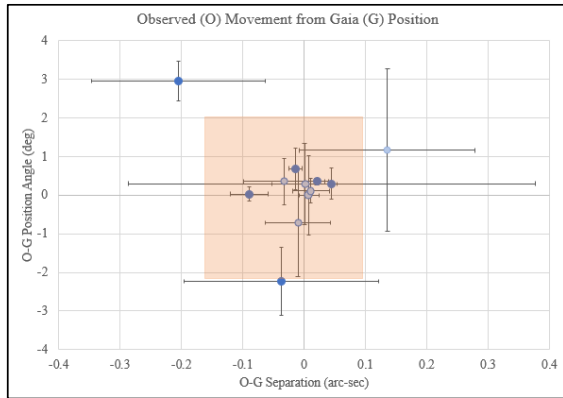

Figure 4. Comparison of the difference between Observed (2020) and Gaia (2015.5) separation and position angles. Uncertainty bars are standard deviations of the observations in Table 2. Solid blue dots indicate possible orbital change in position.
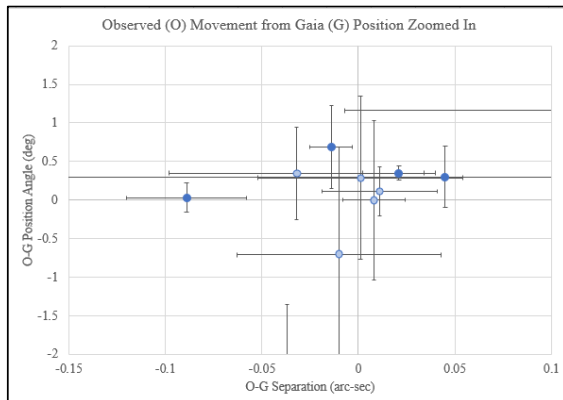

Figure 5. (O-G) data for the stars within the colored box of Figure 4, plotted on an expanded scale. Solid blue dots indicate possible orbital change in position, i.e., greater than 1s uncertainty of r or q, or both.

185453.7+105842 = WDS 18550+1058 = VYS8 is noted as spectral type M0 in the WDS, but the component types—based on the Gaia H-R diagram and (Bp-Rp) colors (1.750/2.586) in Table 1—are roughly K5V and M1V.

This system has the largest movement of all those observed, shown at the upper left of Figure 4: approximately +3.0 ±0.5 degrees in q since the Gaia measurement about five years earlier, or ~0.6°/year. It also has the largest movement since discovery in 1946, about 34° over 74 years, giving a more accurate 0.46°/year. The separation seems to be slowly closing at about -0.02"/year. All the historic data are plotted in Figure 6.

If this motion were part of a circular orbit, it would indicate an orbital period of roughly 780 years. The orbits of all the other systems observed are probably even longer.

Table 1 shows that the Gaia parallaxes and proper motions in RA are nearly identical. However, the proper motions in declination are significantly different; the B component is moving northward at only about 64% the speed of the primary. This is consistent with the direction of motion indicated in Figure 6, but the motion is diagonal, rather than purely north south. This may be the result of orbital motion. This system deserves continued occasional observation, to see whether the roughly linear apparent motion gradually reveals an orbit.
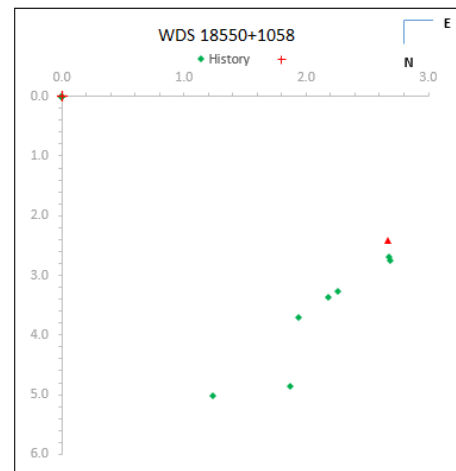

Figure 6. Historical observations of 185453.7+105842 = WDS 18550+1058 = VYS8. The current measure is shown as a red triangle. Since first discovered in 1946, it has shown roughly linear motion, in the direction of the arrow.

For the **191659.0+022216** system, 1-second exposures in r' and i' barely detected the secondary star, as seen in Table 2. It was not detected in the Sloan z' band, even though the exposure was 2 seconds, because of declining detector sensitivity and because it was the most distant observed, at 97 parsecs. Although the secondary star is not a particularly late type M dwarf (Bp-Rp = 2.4), it is very faint at G=14.6. The slightly more faint and much later type RD discussed next was detected in z' with 5 second exposures.

202201.6+214720 is composed of two Red Dwarfs, but of extremely different spectral types. The Gaia color indices from Table 1 are (Bp-Rp) = 2.275/3.716, corresponding roughly to M0V and M7V. Although nearby in the Solar neighborhood at 27pcs, the late component,

**Observations of Potential Gaia DR2 Red Dwarf
Binary Stars in the Solar Neighborhood – II**

G= 14.84, was the faintest star observed; the magnitude difference (DG = 3.57) was also one of the largest observed. Long exposures, 3 seconds in r' and i', and 5 seconds in z', were used to successfully capture this pair with the 11-inch FIRO telescope.

204528.2+370546 is the only system not found in either the WDS or WDSS, so it is truly a new Gaia discovery, not previously data mined or purposely observed. However, it is also a rather peculiar case. The components are similar in Gaia magnitude and color index (Table 1), but the secondary appears much fainter in the images of Table 2, almost disappearing in z' where it should be relatively brighter. Perhaps the secondary star is variable? The proper motions are similar, but the parallaxes are more than 4% different and near the 100 parsecs limit of distance selection in this study. This system deserves further observation.

Conclusion

The objectives of this study were achieved. The observations of Gaia DR2 red dwarf binary stars in the solar neighborhood begun in RDSN-1 was successfully continued in RDSN-2 for 12 more systems that contained a late K or M dwarf star. It was determined that the quasi-speckle interferometry technique could be extended to observations with a telescope of half the aperture and 1/4 the photon-capturing area, reaching about the same faint magnitudes with longer integration times without introducing too much atmospheric smearing. Finally, remote real-time speckle interferometry observational techniques were refined.

We conclude that quasi-speckle interferometry, which employs a single reference star for deconvolution and bispectrum analysis of all observations for phase reconstruction, appears to provide better results than either simple stacking or lucky imaging. This may be due to: (1) the retention of information on the relative position of the two stars in these long-exposure images which can be correlated by speckle processing better than stacking or lucky imaging; (2) single-star deconvolution which can, to some extent, cancel optical aberrations and systematic atmospheric phenomena such as dispersion, and (3) processing of the observations in the Fourier frequency domain which allows suppression of noise at spatial frequencies that cannot be real, e.g., smaller than the Airy disk or larger than the frame size.

Red dwarf secondary stars as late as M7V were observed, but only a few systems showed motion greater than the uncertainties since the observations of Gaia DR2. The fastest moving system, which also happened to have a relatively long observational history (74 years), may have an orbital period on the order of 800 years. Therefore, all these systems likely have long periods.

References

Cooper, K., 2019. "Meet the Neighbors," Sky and Tele scope, January 2019, 35.

Davidson, J., Baptista, B., Horch, E., Franz, O., & van Altena, W., 2009. "A Photometric Analysis of Sev enteen Binary Stars Using Speckle Imaging," The Astronomical Journal, 138, 1354.

Horch, E., Meyer, R., & van Altena, W., 2004. "Speckle observations of Binary Stars with the WIYN telescope—IV. Differential Photometry," The Astronomical Journal, 127:1727–1735.

Marchetti, C., Caputo, R., & Genet, R., 2020. "The Fairborn Institute Robotic Observatory: First Obser vations," submitted to the Journal of Double Star Observations.

Rowe, D., 2018, "GDS1.0 Gaia (DR2) Double Stars Search Program." Private communication.

Rowe, D., & Genet, R., 2015. "User's Guide to PS3 Speckle Interferometry Reduction Program, Journal of Double Star observations, 11, 266.

Wasson, R., Rowe, D., & Genet, R., 2020. "Observation of Gaia (DR2) Red and White Dwarf Binary Stars in the Solar Neighborhood," Journal of Double Star Observations, 16-3, 208.

Winters, J., Henry, T., Jao, W., Subasavage, J., Chate lain, J., Slatten, K., Riedel, A., Silverstein, M., & Payne, M., 2019. "The Solar Neighborhood. XLV: The Stellar Multiplicity Rate of M Dwarfs Within 25 pc," The Astronomical Journal, 157, 216.